Stiffness Assessment through Modal Analysis of an RC Slab Bridge before and after Strengthening

Giovanna Zanardo[1]; Hong Hao, M.ASCE[2]; Yong Xia, Ph.D.[3]; and Andrew J. Deeks[4]

Abstract: As part of Main Roads Western Australia's (MRWA) bridge management and bridge upgrading program, MRWA bridge no. 3014 was assessed to evaluate its condition before and after strengthening works with carbon-fiber-reinforced-polymers (CFRP). The assessment process coupled analytical results with field observations and dynamic testing of the structure. Vibration-based structural assessment of the bridge was conducted before and after the completion of the upgrading works. This paper presents the results of the vibration tests and modal analysis performed before and after the structure upgrading. In particular, the change in the structural properties and stiffness, before and after the strengthening, based on the analyses of the updated models of the bridge, is presented and discussed. The results demonstrate the effectiveness of using the dynamic assessment method to determine the elastic flexural stiffness of bridge structures retrofitted with CFRP.

DOI: 10.1061/(ASCE)1084-0702(2006)11:5(590)

CE Database subject headings: Stiffness; Modal analysis; Slabs; Bridges; Fiber reinforced polymers; Dynamic tests; Assessments.

Introduction

To accurately evaluate the structural condition of bridges and localize their vulnerabilities, information on their construction and operational history must be coupled with in situ investigations. When the bridge can be instrumented, bridge health monitoring (BHM) data, such as field measured static and/or dynamic data, can be used to support the design of strengthening and rehabilitation works, as well as to assess the effectiveness of the retrofit strategies.

There are two main reasons to integrate a "standard" structural assessment with a vibration-based assessment. The first is that a vibration-based assessment can efficiently provide accurate information on the actual performance of the bridge under serviceability conditions. The second is that it allows the identification of certain structural properties, specifically the stiffness (flexibility), damping, and mass. To achieve this dynamic assessment is coupled with model updating. Model updating is an analytical technique in which a numerical model of the structure is adjusted until the computed behavior matches the observed behavior.

There is a large amount of literature on dynamic testing of structures. Many of the recent applications of dynamic testing on bridges provide practically useful information on the assessment process and the identification of the bridge properties (Samman and Biswas 1994a,b; Law et al. 1995a,b; Salawu and Williams 1995; Abdel Wahab and De Roeck 1998; Brownjohn and Xia 2000; Brownjohn et al. 2003; Haritos 2004). However, only in a few instances are the findings of dynamic assessments performed before and after strengthening or upgrade works discussed (Haritos and Chandler 1999; Brownjohn et al. 2003).

It should be noted that since the results are based on experimental studies, they are generally different from one study to another, and apply only to the particular structure tested as well as the specific retrofit strategy applied. Therefore, it is difficult to compare the information available in literature and draw general conclusions on either the accuracy of a certain dynamic assessment procedure or the effectiveness of a particular strengthening procedure.

In this paper, the authors present the findings from a program of dynamic testing and stiffness assessment performed on a four-span reinforced concrete (RC) slab bridge before and after the application of carbon-fiber-reinforced polymers (CFRP) to the top and underside of the bridge deck as strengthening measure. The bridge, MRWA bridge no. 3014, is located in Western Australia and is owned by Main Roads of Western Australia (MRWA).

Significant increase of the capacities of RC bridges after strengthening by CFRP has been reported by Ross et al. (2004). In their study, the effects of the CFRP application on the performance of channel girders under ordinary loads were investigated experimentally. The improvement in the capacity of RC slab bridges after various CFRP applications was confirmed in the assessment of real-life structures by Shahrooz and Boy (2004). They reported the results of the rating of a full-scale three-span RC slab bridge retrofitted with extensive application of different CFRP systems before, shortly after the upgrading works and after one year of service. Controlled truckload tests were performed to evaluate the structural performance.

[1]Lecturer, The Univ. of Sheffield, Dept. of Civil and Structural Engineering, Sir Frederick Mappin Building, Sheffield, S1 3JD, U.K. E-mail: g.zanardo@sheffield.ac.uk

[2]Prof. of Structural Dynamics, School of Civil and Resource Engineering, Univ. of Western Australia, 35 Stirling Highway, Crawley, WA 6009. E-mail: hao@civil.uwa.edu.au

[3]School of Civil and Resource Engineering, Univ. of Western Australia, 35 Stirling Highway, Crawley, WA 6009. E-mail: xia@civil.uwa.edu.au

[4]Prof. and Head, School of Civil and Resource Engineering, Univ. of Western Australia, 35 Stirling Highway, Crawley, WA 6009. E-mail: deeks@civil.uwa.edu.au

Note. Discussion open until February 1, 2007. Separate discussions must be submitted for individual papers. To extend the closing date by one month, a written request must be filed with the ASCE Managing Editor. The manuscript for this paper was submitted for review and possible publication on February 9, 2005; approved on July 15, 2005. This paper is part of the ***Journal of Bridge Engineering***, Vol. 11, No. 5, September 1, 2006. ©ASCE, ISSN 1084-0702/2006/5-590–601/$25.00.

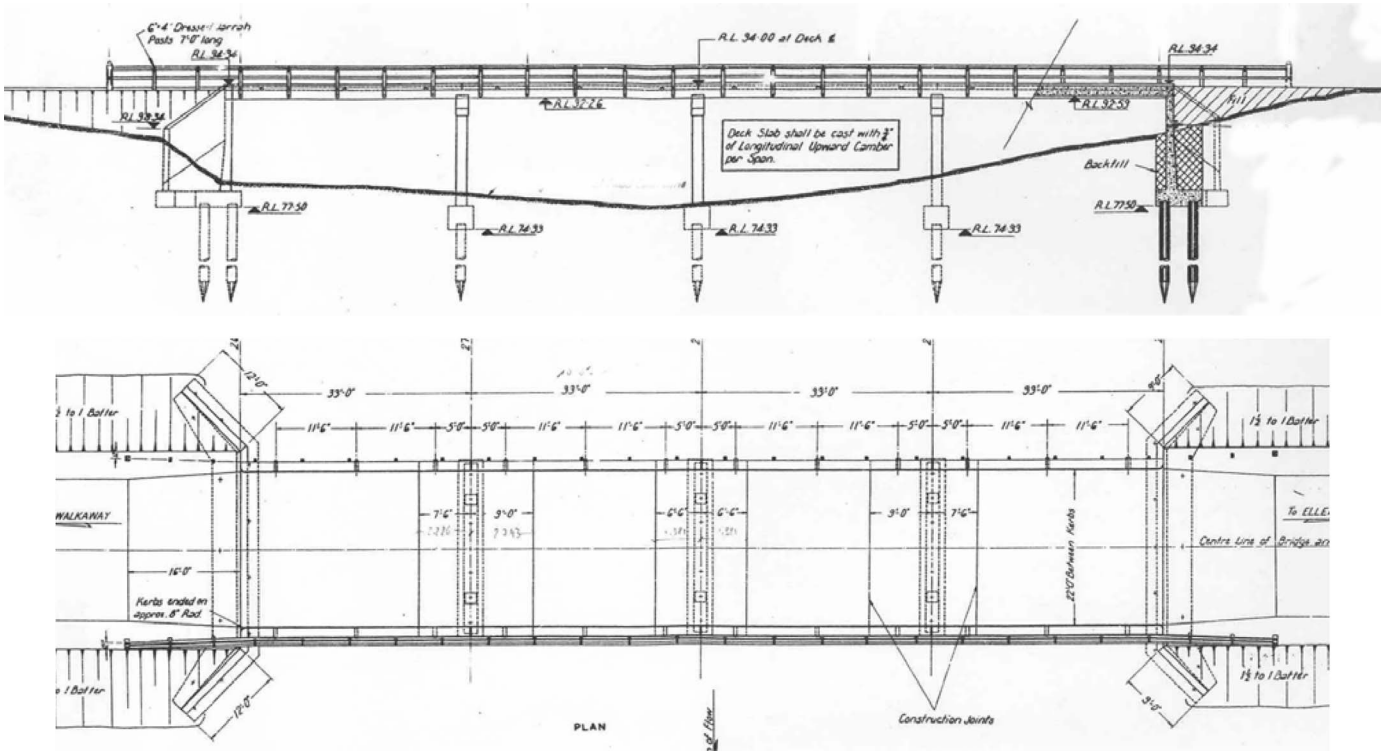

Fig. 1. Bridge views from as-built plans

Regarding the use of vibration-based procedures on the specific assessment of RC slab bridges, Haritos and Chandler (1999) investigated the condition of a full-scale structure, similar in geometry to MRWA bridge no. 3014, through dynamic measurements recorded before and after upgrading works. However, in this case, the retrofit strategy did not include CFRP applications. In another study, Haritos and Hira (2004) evaluated the efficacy of different CFRP strengthening strategies on RC slab bridges through lab tests. However, this study (including a campaign of both static and dynamic tests carried out on 40% reduced-scale models) was oriented toward the identification of the failure mechanisms of the strengthened structures rather than the quantification of the increased stiffness and improved capacity (Haritos and Hira 2004).

No previous study the authors are aware of has evaluated the effectiveness of strengthening a real-life RC slab bridge by CFRP composites through a vibration-based assessment.

The dynamic-based assessment of MRWA bridge no. 3014 was performed in two sessions: before strengthening, to identify any defects in the structure; and after strengthening, to study the effectiveness of the intervention. In this paper, the increase of the structural stiffness after strengthening works is investigated and evaluated through the changes in the modal parameters (such as frequency values and modal shapes) before and after retrofit.

Background

Characteristics of the Structure

Bridge no. 3014 is a four-span continuous RC bridge. The original construction drawings are dated 1963/1964, inferring the structure was probably built in 1964/1965. The bridge is located at SLK 0.87 on Nangetty-Walkaway Road over the Greenough River, in the Shire of Greenough, in Western Australia.

The external spans seat onto abutments on the riverbanks, while the inner spans are situated over the river channel (Figs. 1 and 2). Each span length is 10.06 m and the width is approximately 7.62 m. The width between the curbs is 6.70 m. The average depth of the deck slab is 0.40 m. The deck consists of a RC slab supported on crosshead beams in turn seated on two central piers and RC abutments.

Each of the two piers is founded in the riverbed and consists of two 4.62-m-high RC columns with a 0.50×0.50 m cross section. At the pier base, 1.0-m-high concrete casings increase the column cross section to 0.60×0.60 m. The piers bear on continuous 1.07×7.62 pile cap beams, in turn supported on a line of seven 0.40-m-diameter Jarrah (timber) piles. East and west abutments are continuous RC structures supported on Jarrah piles. At each abutment the bridge supports are allowed to slide longitudinally and transversely, and there are six dowels at 1.22-m centers. The dowel sockets allow horizontal and vertical translations and rotations. At the piers, there are 12 dowels at nominal 0.60-m centers. The dowels are cast into the concrete deck slab at the piers, and therefore are fixed against translation. The connection is essentially pinned, and allows rocking of the support.

The available as-built plans give no indication as to the girder material properties. The material properties of concrete and reinforcement were established after testing of core samples taken from the bridge deck. The mean corrected concrete compressive strength, f_{cm}, was derived from tests performed in accordance with (SAA 1991b; BGE 2001a,b, 2004a,b). The values of f_{cm} as they were obtained from the tests and related to samples taken in different bridge spans are reported in Table 1.

The modulus of elasticity of concrete was calculated as indicated in SAA (2004)

Fig. 2. View of MRWA bridge no. 3014

$$E_c = \rho^{1.5} \times 0.043\sqrt{f_{cm}} \quad (1)$$

where the density of concrete, ρ, determined in accordance with SAA (1998), is given in Table 1. It should be noted that the modulus of elasticity obtained using Eq. (1), whose values are reported in Table 1, has a range of ±20% from this value. This variation was taken into account in the parameter tuning performed for model updating, as discussed later. The steel tensile strength of the bridge was tested in accordance with SAA (1991a) and the test results are given in Table 2.

Structural Condition

Preliminary Assessment

The analytical assessment performed by BG&E (BGE 2001a,b) as consultant to the bridge owner, revealed that the structure did not satisfy the standard requirements for traffic loading and therefore needed strengthening in flexure for both negative (hogging) and positive (sagging) bending moments.

Inspections performed prior to the vibration tests at ground level and close-up investigations of the superstructure confirmed that the structure was exhibiting signs of distress, especially throughout the bridge deck. In particular:

- At both of the bridge ends, large cracks with width varying from 50 to 70 mm were found, with consequent exposure of the coarse aggregate;
- Cracks 5–8-mm wide, principally in the transverse direction of the bridge, were present on the pavement over the piers; and
- The curbs exhibited vertical cracking and reinforcement exposure throughout, especially over the piers.

Preliminary Modeling

"SAP2000/Nonlinear Users Manual" (2000) was used to develop finite element models of the structure. To overcome the difficulties arising when different modeling philosophies are applied, and to test the accuracy of different models, two 3D models of the structure were used in the preliminary analyses. To assess the influence of the stiffness distribution on the bridge vibrational response, both a grillage model (A), which was the model preferred by the bridge owner and its consultant, and a planar slab model (B) were defined to identify the mode shapes.

The grillage method involves the modeling of the bridge slab as a skeletal structure made up of a mesh of beams lying in one plane (West 1973). Each grillage member represents a portion of the slab, with the longitudinal beams representing the longitudinal stiffness and the transverse grillage members representing the transverse stiffness. In model A, the beam section properties were selected to make the grillage equivalent to the RC slab deck. Uncracked concrete section properties were used.

Table 1. Concrete Properties as Derived from Core Samples

SPAN	Location	f_{cm} [MPa]	ρ [kg/m^3]	E [MPa]
1	1/3	43.0	2,400	33,153
1	2/3	45.5	2,400	34,103
2	1/3	40.5	2,400	32,175
2	2/3	45.0	2,400	33,915
3	1/3	41.5	2,420	32,977
3	2/3	43.0	2,400	33,153
4	1/3	44.5	2,420	34,148
4	2/3	48.0	2,420	35,466

Table 2. Reinforcing Steel Properties as Derived from Core Samples

SPAN	Location	Bars	Yield strength f_{sy} [MPa]	Ultimate tensile strength f_{su} [MPa]
1	Midspan	Longitudinal	290	474
2	Midspan	Longitudinal	291	473
3	Midspan	Longitudinal	352	490
4	Midspan	Longitudinal	336	500

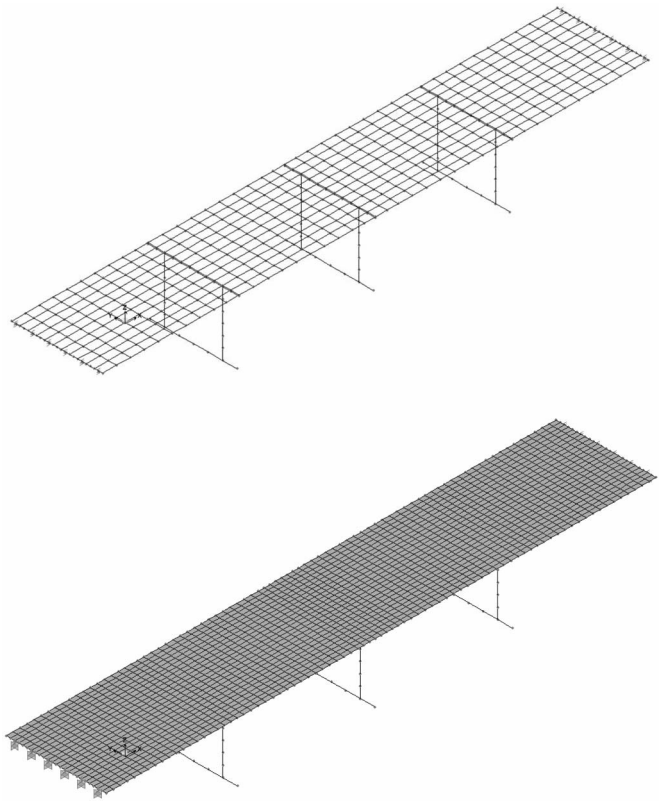

Fig. 3. Preliminary models of the structure: Grillage in model A (top) and slab as system of shell elements in model B (bottom)

In model B, the continuous deck was represented as a fine mesh of isotropic "slab" elements. Shell elements with full shell behavior (membrane and bending action) and uncracked concrete section properties were used.

In both of the models, which are pictured in Fig. 3, the bridge superstructure was represented by a two-dimensional system in which the supports were considered to be at the slab level. The substructure was included and modeled by frame elements representing crosshead beams, columns, and pile cap beams. The piled foundations, including the soil, were represented by linear springs at the pile cap level. The stiffness of the springs representing the Jarrah piles was calculated using the approach of Gazetas (1983), assuming the soil modulus to be constant with depth. Since the piled foundations are in clayey sand, a soil modulus $E_s=40$ MPa was conservatively estimated, while the elastic modulus of the piles was taken as $E_p=14,000$ MPa. Over the piers the deck-pier connections were initially defined as hinges in accordance with the details given in the construction drawings. At the abutments, to represent the boundary condition of possible uplift (but not downward movement of the bridge), compression-only springs were used. The effective stiffness of each of these springs was computed from the abutment properties.

Testing

To calibrate numerical models and accurately evaluate the structural stiffness before and after strengthening, vibration-based assessment of the bridge before and after the upgrading works was conducted. The full-scale dynamic tests were performed in two 2-day sessions carried out on April 15 and 16, 2004, and on August 19 and 20, 2004, before and after the retrofitting.

Fifteen analogue accelerometers were used to measure the bridge dynamic response. The sensors were ADXL 105 5G with a calibration factor of 250 mV/G. Power supply, signal offset, amplification, and filtering for these accelerometers were provided by a 16-channel signal analyzer and a signal generator. An APS 400 electro-dynamic long stroke shaker provided the broadband excitation, while an instrumented sledgehammer was used for shock tests.

Preupgrade Vibration-based Assessment

Sensor Location

All the measurements were performed by fixing the sensors onto the deck surface. Steel plates were fixed to the grid point locations to allow the accelerometers to be magnetically attached. The plates were fixed to the concrete through slugged anchors at locations where the surfacing was rough, and where the surfacing was reasonably smooth, the steel plates were placed on the surfacing without any further anchoring.

A comprehensive set of measurements over the entire structure is required to determine mode shapes. Consequently, measurements of the dynamic response of the bridge were taken over a predetermined grid. The choice of the locations was based on the

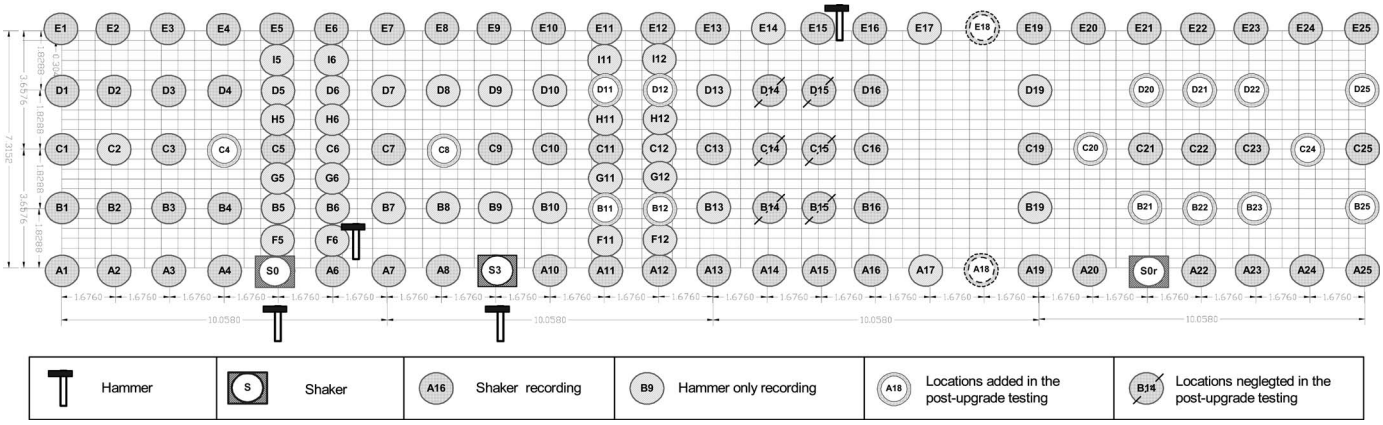

Fig. 4. Grid of sensors locations and points for force application

most likely mode shapes of the bridge under ordinary loads and forced excitation, identified using the preliminary numerical models of the structure. As illustrated in Fig. 4, to allow for identification of the mode shape curvature in the transverse direction, the grid was designed with extra spatial resolution of measurement points at locations 5, 6, 11, and 12. It was planned to keep four sensors in fixed locations as references and to place one sensor on the shaker to record input force, while moving 10 sensors around the other grid points. Measurements on 125 points were planned, but because of difficulties experienced during fieldwork and time constraints, measurements were only recorded on 114 points (see Fig. 4).

Dynamic Measurements

Sine-wave sweep tests were performed, each sweeping from 3 to 30 Hz, and measurements were recorded in frames lasting 32.77 s with a sample rate of 125 Hz.

Usually it is possible for a carefully deployed hammer or impact to excite strong vibrations in all modes (Brownjohn et al. 1999). However, due to difficulty experienced in applying a pure impact, hammer testing at MRWA bridge no. 3014 provided poor quality data, essentially due to a low signal to noise ratio. Only strong local modes were excited resulting in sensor overload, and no useful modal data could be recovered.

The different forms of testing and analyses performed on the structure before the strengthening intervention generated basically the same information: a set of 14 vibration modes in the range 0–30 Hz was identified, essentially bending and torsion mode shapes, with the fundamental frequency at 7.23 Hz. The bending modes showed mainly a half-sine span pattern, while the torsional modes were not particularly complex in the transverse direction of the bridge.

Recovery of Mode Shapes

For each set of n channels and for each measurement (m-point records in n locations), an $m \times n$ matrix of cross-power spectra (CPS) between the response signal from the roving sensors and the excitation was built. The experimental frequency response function (FRF), $H_e(\omega)$, between the excitation and the response was obtained by dividing the entire CPS matrix by the auto-power spectrum of the input signal. In particular, as the only common reference signal between all the measurements was the shaker signal, columns of cross powers with respect to the shaker were extracted from each CPS matrix, normalized by dividing by the shaker auto-power and then combined into a single column. Duplicated data was averaged in this merging.

The analytical form of the FRF, $H(\omega)$, is defined as the rational fraction (Ewins 2000). This "regenerated" FRF (Ewins 2000) was fitted to the measured FRFs to estimate the values of the coefficients such that the error between the analytical FRF and the measured FRF is minimized. The values of the coefficients were then used to estimate the poles and residues of the system, which, in turn, were used to determine the resonant frequencies, modal damping, and mode shapes of the system.

In more detail, following Ewins (2000) the FRF of a linear system with N degrees of freedom (DOF) and viscous damping ξ can be modeled with the following partial fraction equation

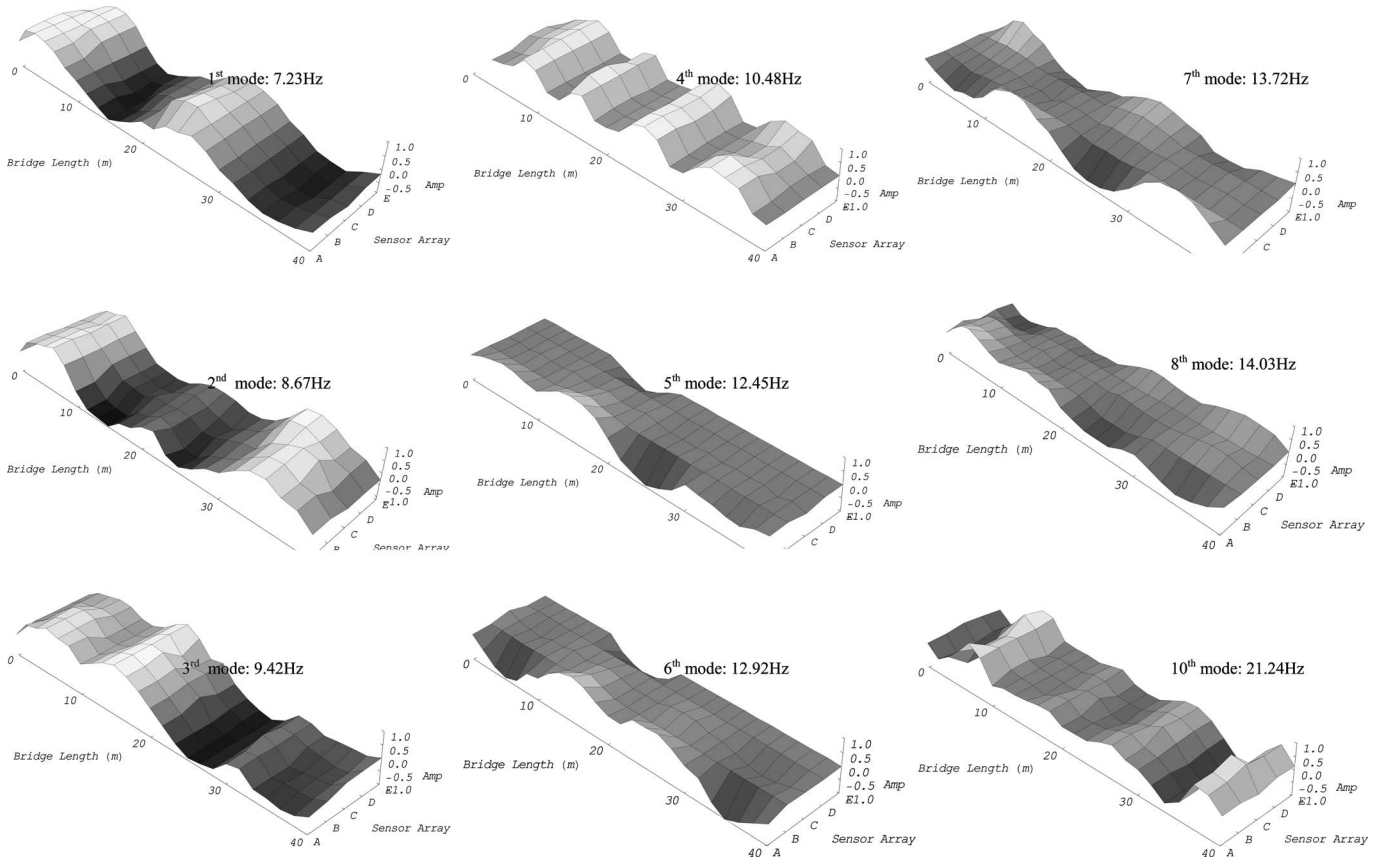

Fig. 5. Preupgrade results: Selected recovered mode shapes

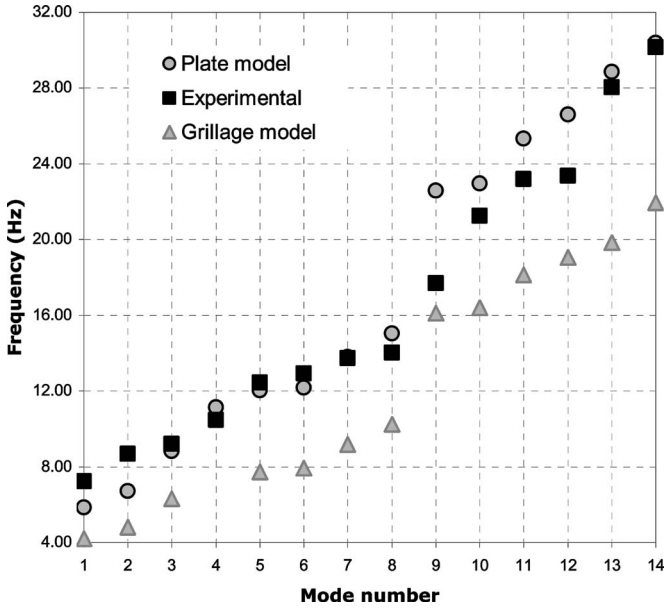

Fig. 6. Preupgrade results: Comparison between experimental and numerical modal frequencies for the plate and grillage models before updating

$$H(\omega) = \sum_{r=1}^{N} \frac{A_r + i\omega B_r}{\omega_r^2 - \omega^2 + 2i\omega\omega_r\xi_r} \tag{2}$$

where A_r and B_r= constants; and ω_r= natural frequency of the rth mode of vibration. It can also be expressed in rational fraction form as

$$H(\omega) = \frac{\sum_{k=0}^{2N-1} a_k(i\omega)^k}{\sum_{k=0}^{2N} b_k(i\omega)^k} \tag{3}$$

The difference between the analytical FRF, $H(\omega)$, and the experimental FRF, $H_e(\omega)$, at measured frequency point ω_j can be quantified by the error function

Table 4. Preupgrade Analyses: Comparison between Updated Analytical (A) and Experimental (E) data

Updated model (A)			Experimental (E)			
Type	Mode	Frequency [Hz]	Mode	Frequency [Hz]	f_A/f_E	Error [%]
First bending	4	7.19	1	7.23	0.994	0.5
Second bending	5	7.98	2	8.67	0.920	7.9
Third bending	6	9.66	3	9.42	0.960	2.5
Fourth bending	7	11.09	4	10.48	1.058	−5.8
—	9	12.93	—	—	—	—
First torsion	10	13.39	5	12.45	1.075	−7.5
Second torsion	11	14.01	6	12.92	1.084	−8.4
Third torsion	12	14.48	7	13.72	1.033	−3.3
Fourth torsion	10	14.01	8	14.03	0.998	0.1
—	13	22.00	—	—	—	—
Fifth bending	14	23.43	9	17.69	1.324	−32.4
Sixth bending	—	—	10	21.24	—	—
Seventh bending	15	25.81	11	23.19	1.113	−11.3
Eighth bending	15	25.81	12	25.37	1.017	−1.7
Fourth torsion loc.	—	—	13	28.03	—	—
Ninth bending	—	—	14	30.16	—	—

$$e_j = \frac{\sum_{k=0}^{2N-1} a_k(i\omega_j)^k}{\sum_{k=0}^{2N} b_k(i\omega_j)^k} - H_e(\omega_j) \tag{4}$$

Summing up the squared error for all measured frequency points, the coefficients a_k and b_k can be found by using the least-squares method to minimize Eq. (4).

Once all the FRFs have been found, these can be analyzed using any standard modal analysis procedure. Fig. 5 illustrates some of the recovered mode shapes.

Model Updating

Comparing the response of the two finite-element (FE) models, the bridge behavior was found to match the slab model better than the grillage model, which is to be expected given the 0.73 ratio between the width and the span length and the higher level of approximation intrinsic in the grillage analogy. A qualitative comparison between the frequencies obtained from the two models before updating is given in Fig. 6.

Table 3. Selected Parameters for the Model Updating

Structural component		Parameter type	Total number of elements	Number of superelements	MIN change in the initial value [%]	MAX change in the initial value [%]
Super-structure	Curbs	EI	24	4	24.3	79.6
	Deck elements	EI	96	6	−8.3	31.1
	Mass density	M_d	144	3	4	5
Structural connections	Pier-deck	K	36	3	Not defined in the initial model	
	Abutment-deck	K	12	1	±35	
Sub-structure	Abutments	K	12	1	±30	
	Foundations	K	18	1	±30	

To perform the updating of model B, an error function ε was considered, defined as the distance of the vector containing the first seven experimental natural frequencies, f_E, from the vector containing the corresponding analytical frequencies, f_A

$$\varepsilon = \sum_{j=1}^{7} \left(\frac{f_E^j - f_A^j}{f_E^j} \right) \tag{5}$$

The frequency error for each mode is divided by the experimental natural frequency, normalizing the contribution of each mode to the total error.

Another useful indicator of correlation between experimental and analytical results used in this study was the modal assurance criterion (MAC), which is defined as (Ewins 2000)

$$MAC(\phi_A, \phi_E) = \frac{|\phi_A^T \phi_E|^2}{(\phi_A^T \phi_A)(\phi_E^T \phi_E)} \tag{6}$$

where ϕ_A and ϕ_E=analytical and experimental modal vectors, respectively. MAC compares experimental and analytical mode shapes and returns a value of unity for perfect correlation, while giving zero for uncorrelated, orthogonal modes.

The parameters selected for the model updating are reported in Table 3. Once their starting values have been selected to be as close as possible to the actual values, a sensitivity-based procedure was applied to define the optimum parameter values. To obtain a reasonable approximation before automatic model tuning, manual tuning of some selected parameters was carried out, particularly to calibrate the stiffness values related to abutments, foundations, and structural connections between the bridge deck and the substructure. Automatic model tuning was then performed.

Table 5. Preupgrade Updating: MAC Values for Initial and Updated Analytical Data (A: analytical; E: experimental)

	Initial model			Updated model		
Type	Mode A	Mode E	MAC	Mode A	Mode E	MAC
First bending	4	1	0.936	4	1	0.977
Second bending	5	2	0.805	5	2	0.853
Third bending	6	3	0.894	6	3	0.943
Fourth bending	7	4	0.810	7	4	0.855
First torsion	11	5	0.953	10	5	0.994
Second torsion	9	6	0.828	11	6	0.900
Third torsion	8	7	0.945	12	7	0.945
Fourth torsion	—	8		10	8	1.000

Results of the preupgrade model updating are reported in Table 4, where the error is normalized by the experimental values. It should be noted that the results are ordered starting from the first mode shape recovered from the postupgrade measurements (bending). All recovered modes are numbered in a sequential order, according to the sequence they appeared after using the shaker or hammer only. On the other hand, through the FE analy-

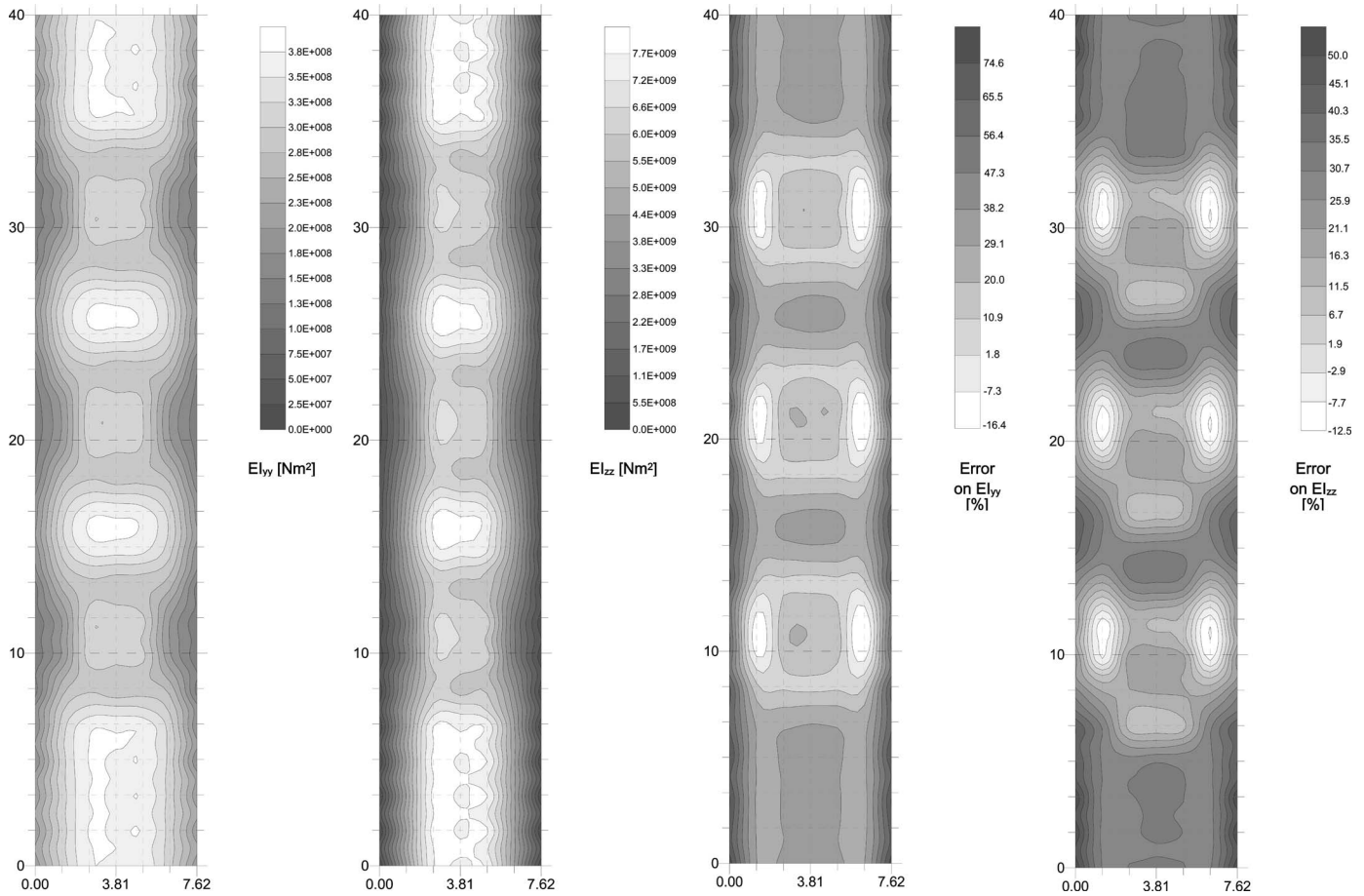

Fig. 7. Preupgrade results: Distribution of stiffness and related error after updating (bridge dimensions in m)

Table 6. CFRP Properties

Fiber type	Carbon
Thickness t_f (mm)	0.14/2.40
Elastic modulus E_f (GPa)	150–200
Ultimate strain ϵ_{fu}(%)	1.4
Characteristic tensile stress at rupture f_{fu} (MPa)	>2,200

sis, all possible mode shapes of the analytical model are calculated, and the total number recovered depends on the number of degrees of freedom of the model.

The FE model of the structure was defined by dividing the bridge superstructure, substructure, and structural connections into a number of elements. To minimize the number of parameters to be considered in the model updating, when finite elements of the same typology and properties were used, in the updating procedure they were grouped into sets of elements called *superelements*. All defined superelements (i.e., sets of elements with identical properties) are detailed in Table 3. The model updating was performed by tuning the superelements properties.

To match the sequence of the modes as they appeared from experimental data, as well as to adjust the mode shape configuration at the bridge ends, the actual cross sections of the curbs was represented by beam elements. To account for their different properties in different locations, four curb superelements were introduced. The variation of the bending stiffness *EI* of the deck slab was described through the definition of six shell superelements. The local change in mass density was taken into account through the incorporation of mass elements. To represent the uneven surfacing on the deck, three mass superelements with different values of mass density were defined in different deck locations.

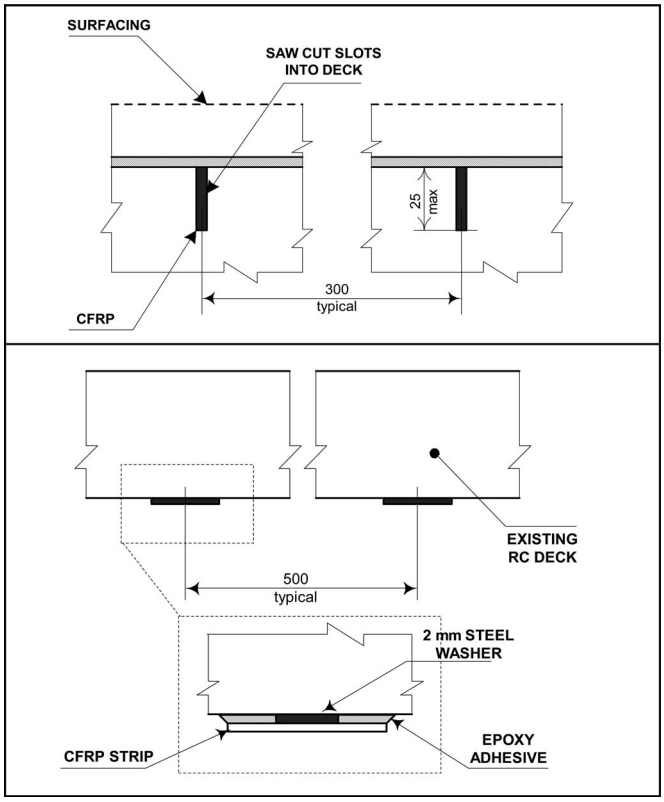

Fig. 8. Details on the application of CFRP laminate strips on the slab soffit and on the top of the deck

Table 7. Postupgrade Results: Young's Modulus Values Computed for the Deck Elements after Updating

		E[MPa] Location					
	Element	K	A	B	C	D	K
Span#1	1	36,000	37,628	37,628	37,628	37,628	36,000
	2	36,000	37,628	37,628	37,628	37,628	36,000
	3	30,185	37,628	37,628	37,628	37,628	30,185
	4	28,576	37,628	37,628	37,628	37,628	28,576
	5	21,873	36,965	37,225	37,225	36,965	21,873
	6	21,873	38,717	36,965	36,965	38,717	21,873
Span#2	7	22,885	37,207	35,523	35,523	37,207	22,885
	8	24,173	35,523	35,773	35,773	35,523	24,173
	9	30,185	36,161	36,161	36,161	36,161	30,185
	10	28,576	36,161	36,161	36,161	36,161	28,576
	11	21,873	35,523	37,225	37,225	35,523	21,873
	12	21,873	38,717	35,523	35,523	38,717	21,873
Span#3	13	22,885	37,002	35,327	35,327	37,002	22,885
	14	24,173	35,327	35,576	35,576	35,327	24,173
	15	30,185	35,961	35,961	35,961	35,961	30,185
	16	28,576	35,961	35,961	35,961	35,961	28,576
	17	21,873	35,327	35,576	35,576	35,327	21,873
	18	21,873	37,002	35,327	35,327	37,002	21,873
Span#4	19	22,885	37,633	35,930	35,930	38,717	22,885
	20	24,173	35,930	36,183	36,183	35,930	24,173
	21	30,185	36,575	36,575	36,575	36,575	30,185
	22	35,986	36,575	36,575	36,575	36,575	35,986
	23	36,000	36,575	36,575	36,575	36,575	36,000
	24	36,000	36,575	36,575	36,575	36,575	36,000
		Curb			Deck		Curb

Note: Each span is divided into a 6×6 grid of subelements.

K refers to curb elements. A, B, C, and D refer to location on the inner part of the deck.

Connections between the deck and the piers were grouped into three main superelements. All bearings located on the piers were represented through link elements of a single type. Both vertical and lateral components of the link stiffness were specified to take into account of the flexibility of the dowels connecting the piers to the deck.

No further change was necessary in the representation of the abutment–deck connections and piled foundations. All supports over the abutments were found to have similar properties and one type of link element was found to be sufficient. Similarly for pile modeling, all springs could be specified using a single stiffness value.

The effect on the error function ε of the inclusion of curbs and uneven surfacing was found to be relatively small. On the other hand, the bending stiffness of the deck superelements, the stiffness of the structural connections, and piled foundation superelements were found to be the key parameters affecting the modal response of the FE model at different frequencies. Consequently these were the best ones to improve the correlation between analytical and experimental modal shapes (as demonstrated by the MAC values reported in Table 5).

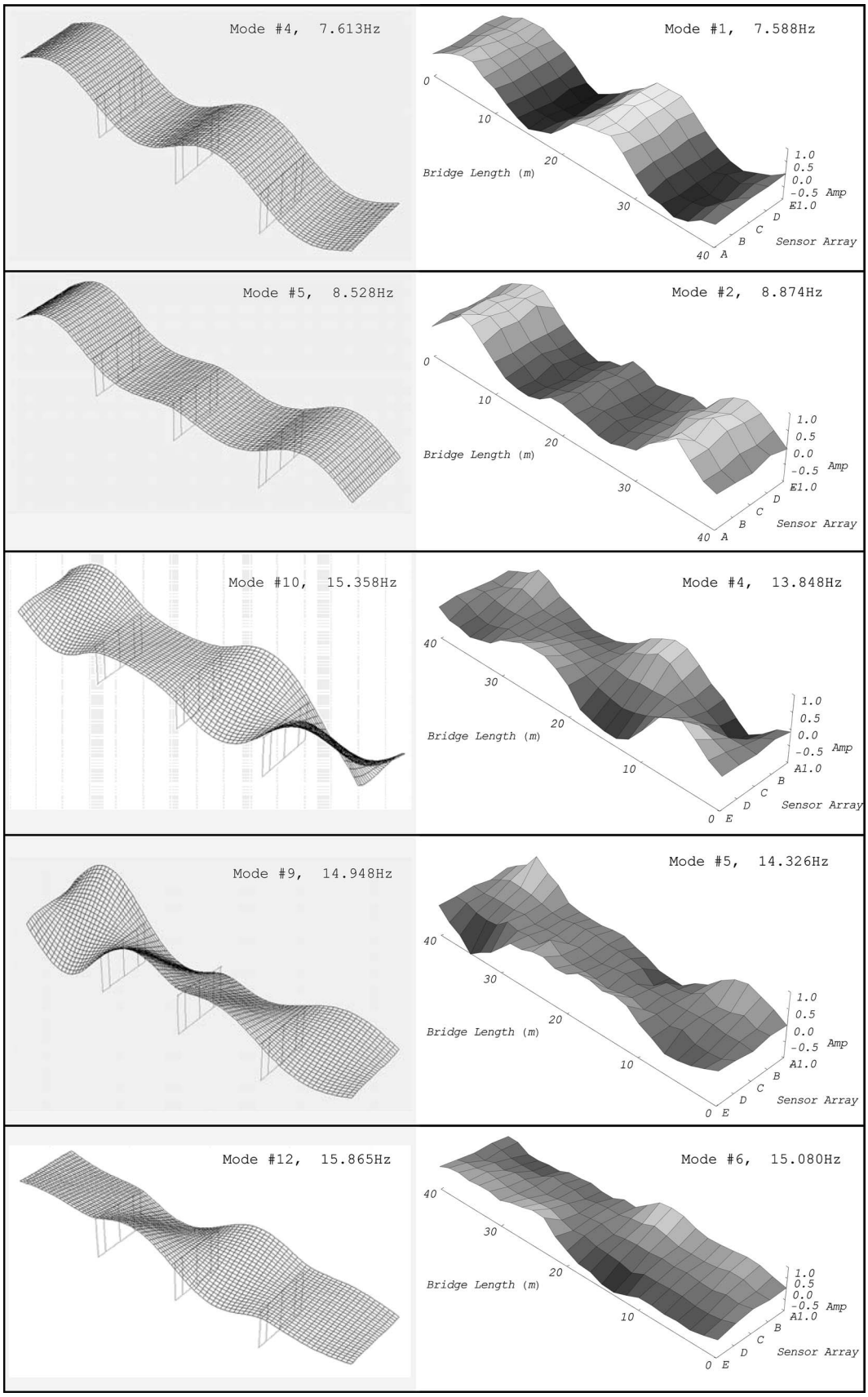

Fig. 9. Postupgrade results: Selected recovered mode shapes (right) compared with the analytical equivalents

Table 8. Postupgrade Results: MAC Values before and after Model Updating

Mode	Type	Initial model	MAC	Updated model	MAC
1	First bending	4	0.903	4	0.917
2	Second bending	5	0.885	5	0.921
4	First torsion	11	0.806	10	0.813
5	Second torsion	10	0.675	9	0.872
6	Fourth torsion	12	0.771	12	0.918

Preupgrade Findings

After model updating, the analytical model showed that the bridge deck stiffness was significantly lower than that approximated from the as-built plans of the structure (Zanardo et al., 2004). The distribution of stiffness and the associated error after model updating are shown graphically in Fig. 7. The error in the initial calculation of the stiffness, EI_i, is presented normalized by the values obtained after updating, EI_u, and it is calculated as $(EI_i - EI_u)/EI_u$.

Postupgrade Dynamic-Based Assessment

Retrofit Strategy

To increase the load-carrying capacity and to maintain it over the expected operational life of the structure, strengthening works were proposed by BG&E (BGE 2004a, b). These works consisted of the application of CFRP laminate strips (see properties in Table 6) to the slab soffit and to the top of the deck over the pier supports (Fig. 8).

To reduce the high negative bending moments, CFRP laminate strips were bonded inside vertical slots on the top of the deck over the piers (near-surface mounted). Each strip cross-sectional area is 2.4×20 mm; the strips are 4-m long and are spaced at 300-mm centers. To reduce the high positive bending moments, CFRP 8.06-m-long laminate strips were applied to the deck soffit in the midspan regions (surface mounted). These strips were bonded directly to the slab underside. Each strip cross-sectional area is 1.4-mm thick $\times$ 80-mm wide and the strips are spaced at 500-mm centers (BGE 2004a,b).

All CFRP strips were bonded to the deck in accordance with the manufacturer's requirements and recommended practices.

Table 9. Comparison between Experimental (E) and Updated Analytical (A) Data, before (1) and after (2) Upgrading

Experimental Preupgrading (1)		Experimental Postupgrading (2)		
Mode type	Frequency f_{E1} [Hz]	Frequency f_{E2} [Hz]	f_{E2}/f_{E1}	Difference
First bending	7.23	7.59	1.049	4.9%
Second bending	8.67	8.74	1.008	0.8%
First torsion	13.72	13.85	1.042	0.9%
Second torsion	12.92	14.32	1.093	10.8%
Fourth torsion	14.03	15.08	1.051	7.4%
Analytical Preupgrading (1)		Analytical Postupgrading (2)		
Mode type	Frequency f_{E1} [Hz]	Frequency f_{E2} [Hz]	f_{E2}/f_{E1}	Difference
First bending	7.19	7.61	1.052	5.2%
Second bending	7.98	8.53	1.069	6.8%
First torsion	13.89	15.36	1.106	10.6%
Second torsion	14.01	14.95	1.093	6.7%
Fourth torsion	14.48	15.16	1.047	4.7%

Table 10. Maximum Increase in Flexural Stiffness Due to Retrofit in Some Locations (Data Derived after Model Updating)

	(Postupgrade)-(Preupgrade)	
Location	EI_{yy} [Nm^2]	EI_{zz} [Nm^2]
A	26%	5%
B	32%	31%
C	32%	31%
D	26%	5%
K	0%	0%

Note: K refers to curb elements.
A, B, C, and D refer to locations on the inner part of the deck.

Testing

The vibration response was recorded in 134 locations to allow greater resolution of the mode shapes than was possible in the preupgrade testing. Preliminary assessment of the bridge vibration properties identified the dominant frequency range as 5 to 45 Hz. A sequence of measurements with accelerometers arranged as shown in Fig. 4 was performed using a combination of shaker excitation and hammer impact to provide sufficient quality data for system identification.

After the testing exercise, the following conclusions were drawn:

- Hammer impact was not effective because of the use of an excessively hard head; and
- Running the shaker using a chirp signal from 5 to 45 Hz in frames of 131.07 s sampled at 125 Hz was the best means of producing useful data.

Model of the Postupgrade Structure and Model Updating

In the postupgrade model, the addition of CFRP laminate strips to the deck slab was simulated by the addition of frame elements to the shell elements representing the bridge deck in model B. Frame elements were added on both the upper side and underside of the shell plane. The geometry of the CFRP elements was defined by the strengthening design as illustrated in Fig. 8 and as previously described.

In updating the post-upgrade model, the elasticity moduli of both the CFRP and shell elements were identified as the most important parameters. They were varied until reasonable agreement with the experimental data was reached in each vibration mode for the assessed dominant frequencies. The elastic modulus of the CFRP elements was restricted to the bounds indicated by the manufacturer (Table 6).

Where discrepancies were found, the stiffnesses of the shell superelements were recalculated allowing (as a consequence of the CFRP application) a uniformly distributed increase of strength of the RC slab elements. Given the substantially unchanged inertia properties of the superstructure sections after strengthening,

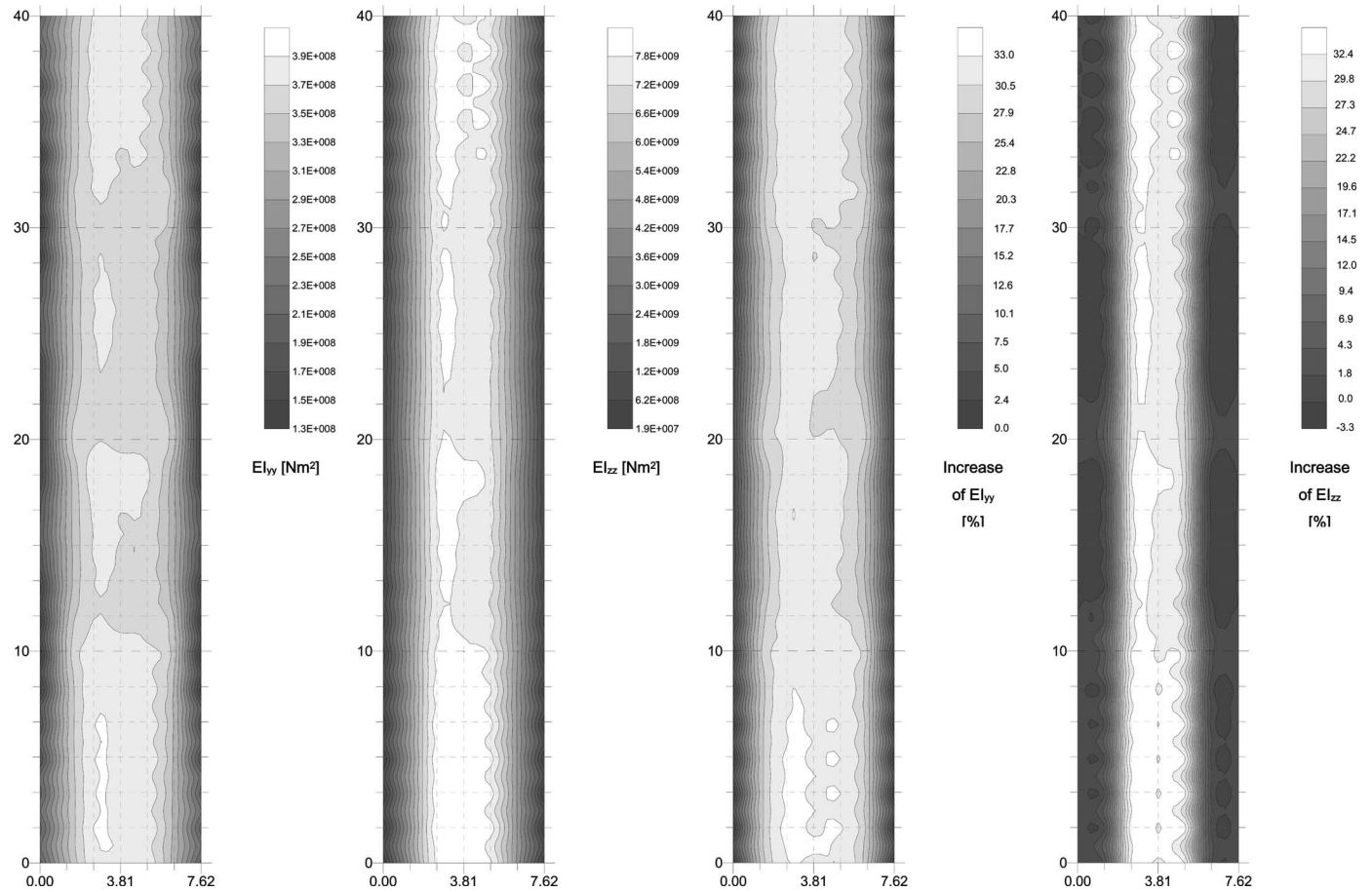

Fig. 10. Postupgrade results: Distributed of stiffness and related increase after updating (bridge dimensions in m)

the strength increase was computed in terms of an increase of the elastic modulus of the shell elements, which was previously derived from the modulus of elasticity of concrete and the grade of reinforcement. A satisfactory correlation with the field measurements was achieved after adjusting the Young's modulus of the deck shell elements to the values reported in Table 7. The mode shapes of the calibrated model of the retrofitted bridge are compared to the measured mode shapes in Fig. 9, while the associated MAC values are reported in Table 8.

Like the preupgrade analyses, the results are tabulated starting from the first mode shape recovered from the postupgrade measurements (bending). All recovered modes are numbered sequentially. The analytical values of the modal frequencies reported in the table are ordered so that the analytical mode shapes best match the corresponding mode shapes recovered from the experimental data. These appear generally in increasing order. Five of the vibration modes derived from processed data were used for updating the model of the structure after upgrade.

Comparison of the Structural Performance before and after Strengthening

Comparisons between the experimentally determined modal properties of the original and strengthened structure and the resulting updated numerical models allow detailed information on the bridge condition to be derived, particularly in terms of overall and local increase of the superstructure stiffness after the CFRP application.

The modal frequencies before and after upgrading works are compared in Table 9. Notably the upgrading works resulted in a change of about 5% in the experimental first mode frequency, while the change appears to be more significant for higher experimental torsional mode frequencies (up to 10%). Similarly, after the model updating, in the updated analytical model of the structure after strengthening, the fundamental frequencies increased by 4.7 to 10.6%. This change in the frequency values indicates increase in the structural stiffness.

In fact, despite the relatively small changes in the vibration properties of the structure, the analytical model matched the experimental data only after the inclusion of CFRP elements in the system and modifications of up to 5.0% of the material properties defined for the superstructure shell elements (see Table 8). As a consequence, the model updating indicated that the structural stiffness was generally enhanced, and in certain local areas of the superstructure the stiffness increase was significant. In Table 10, where local maximum and minimum values of the flexural stiffness after retrofit are reported, the maximum increase of 32% refers to superstructure elements located over the piers. The final results in terms of both stiffness distribution and stiffness increase are illustrated in Fig. 10.

Every bridge assessment depends on a large number of parameters, and the results can only be verified in the particular context considered. However, these results are consistent with a similar RC bridge where the concrete strain was reported to have reduced by about 34% after strengthening (Shahrooz and Boy 2004).

Conclusions

This paper shows how the elastic flexural stiffness of bridge structures retrofitted with CFRP can be evaluated through dynamic-based assessment procedures. To the authors' knowledge this is the first reported investigation where the assessment of the effects of deck strengthening by CFRP on the performance of RC bridge structures has been performed through the analysis of dynamic measurements. A main conclusion of the presented study is that dynamic measurements provide valuable support to the understanding of the changes in structural behavior before and after strengthening by CFRP. Consequently, dynamic measurements are a powerful instrument to calibrate and optimize the design of these strengthening interventions.

Acknowledgments

The authors would like to thank Adam Lim and Jock Scanlon of MRWA and Peter Coughlan of BG&E for providing the structural information for MRWA bridge no. 3014, the assistance and support during the testing sessions, and the opportunity for carrying out a dynamic-based assessment of the structure. Many thanks to Minhdu Nguyen, Craig Boston, Jim Waters, Alex Duff, and Wayne Galbraith for their help in the test preparation and on-site work. Partial financial support from the Australian Research Council, under grant LP0453783, is also acknowledged.

References

Abdel Wahab, M. M., and De Roeck, G. (1998). "Dynamic testing of prestressed concrete bridges and numerical verification." *J. Bridge Eng.*, 3(4), 159–169.

BGE. (2001a). "Bridge no. 3014 on Walkaway-Nangetty Road over Greenough River, shire of Greenough—Load rating report." Ref. 10369.04-004/3014 Rev 1, BG&E, Perth, WA, Australia.

BGE. (2001b). "Engineering report on material testing and the implications to rated load capacity for bridges 795, 205 and 3014." Ref. 10369.04-005 Rev 0, BG&E, Perth, WA, Australia.

BGE. (2004a). "Bridge no. 3014, Walkaway-Nangetty Road, midwest region, shire of Greenough—work summary report." Ref. 11285.00-037/3014 Report N. 01 Rev A, BG&E, Perth, WA, Australia.

BGE. (2004b). "Engineering report on additional material testing of reinforcing steel for bridges 795, 205 and 3014." Ref. 10369.04-008 Rev 0, BG&E, Perth, WA, Australia.

Brownjohn, J. M. W., Lee, J., and Cheong, B. (1999). "Dynamic performance of a curved cable-stayed bridge." *Eng. Struct.*, 21(11), 1015–1027.

Brownjohn, J. M. W., Moyo, P., Omenzetter, P., and Yong, L. (2003). "Assessment of highway bridge upgrading by testing and finite-element model updating." *J. Bridge Eng.*, 8(3), 162–172.

Brownjohn, J. M. W., and Xia, P. Q. (2000). "Dynamic assessment of curved cable-stayed bridge by model updating." *J. Struct. Eng.*, 126(2), 252–260.

Ewins, D. J. (2000). *Modal testing—Theory, practice and application*. Research Studies Press Ltd. Baldock, Hertfordshire, U.K.

Gazetas, G. (1983). "Analysis of machine foundation vibrations: State-of-the-art review." *Int. J. Soil Dyn. Earthquake Eng.*, 2(1), 2–42.

Haritos, N. (2004). "Assessing the characteristics of structural systems using dynamic testing." *Proc., 18th Australasian Conference on the Mechanics of Structures and Materials*, Vol II, 1211–1217.

Haritos, N., and Chandler, I. (1999). "Structural identification of MRWA bridge 617." *Mechanics of structures and materials*, Bradford, Bridge, and Foster, Eds., Balkema, Rotterdam.

Haritos, N., and Hira, A. (2004). "Repair and strengthening of RC flat slab bridges using CFRPs." *Compos. Struct.*, 66, 555–562.

Law, S. S., Ward, H. S., Shi, G. B., Chen, R. Z., Waldron, P., and Taylor, C. A. (1995a). "Dynamic assessment of bridge load-carrying capacities. Part I." *J. Struct. Eng.*, 121(3), 478–487.

Law, S. S. Ward, H. S., Shi, B. B., Chen, R. S., Waldron, P., and Taylor, C. A. (1995b). "Dynamic assessment of bridge load-carrying capacities: Part II." *J. Struct. Eng.*, 121(3), 488–495.

Ross, S., Boyd, A., Johnson, M., Sexsmith, R., and Banthia, N. (2004). "Potential retrofit methods for concrete channel beam bridges using glass fiber reinforced polymer." *J. Bridge Eng.*, 9(1), 66–74.

Salawu, O. S., and Williams, C. (1995). "Bridge assessment using forced vibration testing." *J. Struct. Eng.*, 121(2), 161–172.

Samman, M. M., and Biswas, M. (1994a). "Vibration testing for nondestructive evaluation of bridges. Part I: Theory." *J. Struct. Eng.*, 120(1), 269–289.

Samman, M. M., and Biswas, M. (1994b). "Vibration testing for nondestructive evaluation of bridges. Part II: Theory." *J. Struct. Eng.*, 120(1), 290–306.

SAP2000/Nonlinear Users Manual. (2000). *Comput. Struct.*, Berkeley.

Shahrooz, B. M., and Boy, S. (2004). "Retrofit of a three-span slab bridge with fiber reinforced polymer systems—Testing and rating." *J. Compos. Constr.*, 8(3), 241–247.

Standards Association of Australia (SAA). (1991a). "Methods for tensile testing of metals." SAA, Sydney, NSW, Australia.

Standards Association of Australia (SAA). (1991b). "Methods of testing concrete—Method 14: Method for securing testing cores from hardened concrete for compressive strength." SAA, Sydney, NSW, Australia.

Standards Association of Australia (SAA). (1998). "Methods of testing concrete—Method 12: Determination of mass per unit volume of hardened concrete." SAA, Sydney, NSW, Australia.

Standards Association of Australia (SAA). (2004). "Bridge design—Part 5: Concrete." SAA, Sydney, NSW, Australia.

West, R. (1973). "Recommendations on the use of grillage analysis for slab and pseudo-slab bridge decks." *Cement and Concrete Association*, C&CA/CIRIA, London.

Zanardo, G., Hao, H., and Deeks, A. J. (2004). "Dynamic-based assessment of MRWA bridge no. 3014." *Proc., 18th Australasian Conference on the Mechanics of Structures and Materials*, Vol. II, Perth, WA, Australia, 1231–1237.